Eurasian Journal of Science Engineering and Technology

Research Article

LARGE-SCALE SYNTHESIS OF HOMOGENEOUS WS_2 FILMS BY PHYSICAL VAPOR DEPOSITION

Ali ALTUNTEPE[1],*, Serkan ERKAN[2], Güldöne KARADENİZ[3]

[1,2,3] *Nigde Omer Halisdemir University, Nanotechnology Research and Application Center, 51240, Niğde, Türkiye*

ABSTRACT

TMDs are semiconductors, unlike graphene, and have a direct bandgap when converted from bulk to thin film. This property makes TMDs an ideal material for optoelectronic and photovoltaic applications due to their strong optical absorption and photoluminescence effect. The WS_2, a popular TMD, has unique properties such as low friction coefficient, high thermal stability, and good electrical conductivity, and a bandgap energy of approximately 1.2 eV and 2.2 eV for indirect and direct behaviors. The article also discusses various methods for synthesizing WS_2, including chemical vapor deposition (CVD), physical vapor deposition (PVD), hydrothermal synthesis, and solvothermal synthesis. PVD is a scalable method for producing large-area films and coatings with high quality, but the difficulty of controlling the sulfur or selenium sources in this method leads to the need for optimizing growth parameters for large-scale and high-quality WS_2 film synthesis. The study reports the successful growth of large-scale and homogeneous WS_2 films on a glass substrate using PVD and optimized substrate temperature. The results of this study provide valuable information for the advancement of WS_2 film growth techniques and the development of WS_2-based semiconductor technologies, such as transistors, diodes, photodetectors, and solar cells.

Keywords: WS_2, PVD, Substrate temperature

1. INTRODUCTION

Since the isolation of graphene, the first 2D material with superior electrical, chemical and mechanical properties, interest in the synthesis, characterization and application of graphene and other 2D materials has rapidly increased [1, 2]. The outstanding optical properties like light transmittance and energy band gap of graphene and 2Ds, and in particular those of TMDs, have been promising for the use of these materials in energy and photovoltaic applications, and studies in this field have intensified [3]. The TMDs known to have MX_2 (M: Mo, W; X: S, Se, Te) structure are semiconductors in contrast to the semi-metal nature of graphene and when they are converted from bulk form to thin film, the indirect band gap becomes direct band gap [4]. This transition leads to a strong optical absorption by creating a large photoluminescence effect in the material which is one of the main reasons why TMDs are preferred for optoelectronic and photovoltaic applications. The estimated about 10% absorbance value of monolayer TMDs in the visible region corresponds to 50 nm thick silicon commonly used in solar cell applications. However, while it can produce 2.0−4.5 mA/cm^2 photocurrent, this value is limited to about 0.1 mA/cm^2 for the silicon of approximately similar thickness [5]. In addition, TMDs have been prominent and popular thanks to their band gap energy, which can be modified by doping and adjusted to a desired level. This has paved the way for TMDs to be used in many semiconductor technologies such as transistors, diodes, photodetectors, and solar cells [6].

The WS_2 is one of the most popular 2D materials in among TMDS because of it has attractive properties. The WS_2 has a layered structure, with each layer consisting of a sheet of tungsten atoms sandwiched between two layers of sulfur atoms. The layers are held together by weak Van der Waals forces. This layered structure gives WS_2 its unique properties such as its low friction coefficient, high thermal stability, and good electrical conductivity. The WS2 material has an approximately 1.2 eV and 2.2 eV band gap for indirect and direct behaviors, and a mobility value of about 150 $cm^2\ V^{-1}\ s^{-1}$ has an n-type property [7]. The WX_2 group, has the lowest bandwidth among TMDs with a 1.1 eV bandwidth [8]. Moreover, its having p-type features allows homo and hetero PN junction structures to be obtained. More specifically, the mentioned TMDs' property regarding having different band gap values enables the development of open circuit voltage (Voc), which is an important parameter in solar cell applications. WS_2 can be synthesized using several methods, including chemical vapor deposition (CVD), physical vapor deposition (PVD) hydrothermal synthesis, mechanical exfoliation, solvothermal synthesis, and sulfurization of tungsten [2]. PVD is a versatile and scalable method that can produce large-area films and coatings with high quality [9]. Hydrothermal synthesis and solvothermal synthesis are relatively simple and low-cost methods but typically result in lower-quality WS_2 compared to PVD. Although PVD method provide large area film growth difficulty of controlling S or Se sources in this method [10]. Therefore, growth parameters should be optimized to homogeny and high quality WS_2 films growth.

* Corresponding author, e-mail: altuntepeali@gmail.com (A. Altuntepe)
Recieved: 24.05.2023 Accepted: 09.06.2023
doi: 10.55696/ejset.1301601

In this study, large scale and homogeneous WS_2 films were growth. The WS_2 films were growth on the glass substrate with the PVD system and by optimizing the substrate temperature of RT, 300 °C, 400 °C, and 500 °C. Optimum substrate temperature was determined to obtain large scale and high quality WS_2 film synthesis. The results of the study provide valuable information for the development and improvement of WS_2 film growth techniques, which can ultimately lead to the advancement of the technology.

2. MATERIAL AND METHOD

In this study, we investigated substrate temperature effect on the WS_2 growth by PVD (RF sputtering) methods. All growth processes were given in Table 1. For this aim, glass used as a substrate and cleaning processes applied to substrate before growth process. First of all, all substrates were cleaned with Acetone, IPA, and DW with 10 min, 10 min, and 20 min in the ultrasonic bath, respectively. After this, all substrates were dried with N_2 gas flow. The ultrasonic plasma cleaner was used at last step of the cleaning process for removed remaining contaminants. The magnetron sputtering was carried out at 15 nm film thickness with RF power of 50 Watt at a sputtering base pressure of $1.6x10^{-6}$ Torr and growth pressure of $3x10^{-3}$ Torr in a pure Ar gas atmosphere. The 15 nm thick WS_2 films coated by RF sputtering method at room temperature (RT), 300 °C, 400 °C and 500 °C substrate temperature with deposition rate of 0.2 Å/s.

Table 1. Cleaning and growth process of WS_2

Cleaning Process		**Growth Process**	
Acetone	10 min.	**Base Pressure**	$1.6x10^{-6}$ Torr
IPA	10 min.	**Growth Pressure**	$3x10^{-3}$ Torr
DW	20 min.	**RF Power**	50 Watt
Dried	Ar gas	**Deposition Rate**	0.2 Å/s
Ultrasonic Plasma Cleaner	20 min.	**Temperature**	RT, 300 °C, 400 °C, 500 °C

The structural properties of WS_2 films were characterized by Raman spectra and scanning electron microscope (SEM) measurements. In addition, the optical properties were determined with ellipsometer and photoluminescence spectroscopy (PL).

3. RESULTS AND DISCUSSION

The Raman spectra of 2D WS_2 films grown at RT, 300, 400 and 500 °C substrate temperature and exposed to a 532 nm laser are shown in Figure 1. The first-order Raman modes of WS_2 films at the Brillouin zone center were attributed to E_{2g}^1 and A_{1g} modes. The E_{2g}^1 mode corresponds to the transversal movement of W and S atoms in the lattice, while the A_{1g} mode corresponds to the longitudinal movement of these atoms. In addition, the longitudinal acoustic phonons 2LA(M), which denote in-plane collective movements of atoms in the WS_2 lattice, and other WS_2 modes were labeled in the graph. The E_{2g}^1 and A_{1g} modes were observed at approximately 354 cm^{-1} and 418 cm^{-1} for RT, 300 °C and 400 °C substrate temperatures. However, the E_{2g}^1 mode was not observed for 500 °C. This indicates that the 2LA(M) and E_{2g}^1 modes overlapped at approximately 352 cm^{-1}, and the A_{1g} mode was detected at around 418 cm^{-1}. Furthermore, at a 400 °C substrate temperature, the 2LA(M) and E_{2g}^1 mode overlapped at approximately 354 cm^{-1}. The intensity of the LA(M) increased while that of the A_{1g} decreased with a reduction in the number of layers of 2D-WS_2 films. The Raman spectra showed that the 400 °C sample tended to grow as a few layers, while the other samples exhibited multi-layer or bulk behavior.

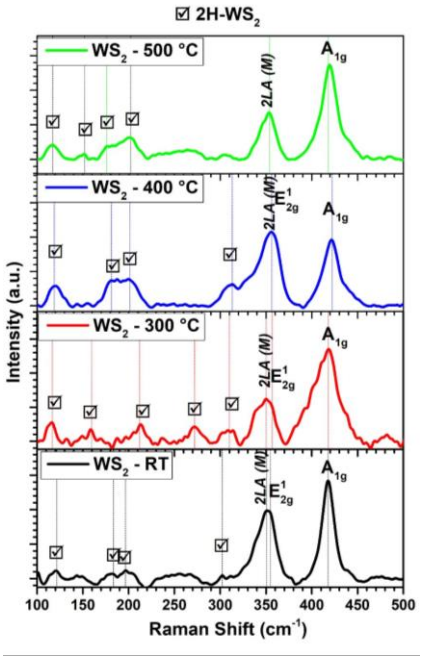

Figure 1. Raman spectra of 2D-WS_2 films growth with RT, 300, 400, and 500 °C substrate temperature

The PL measurements of 2D-WS_2 grown at RT, 300°C, 400°C and 500°C substrate temperature are shown in Figure 2. The bulk WS_2 exhibits PL emission at around 1.2 eV as an indirect band transition in the literature [11]. In Figure 2, the sample of RT, 300 °C, and 500 °C substrate temperature showed approximately 1.25 eV PL emission that situation attributed to the indirect band transition. The statement indicates that the photoluminescence (PL) intensity of bulk samples is very weak. This finding is in line with the behavior of an indirect bandgap semiconductor in its bulk form. An indirect bandgap material has a lower efficiency in emitting light compared to a direct bandgap material. Therefore, the weak PL intensity observed in bulk samples suggests that the emission of light is less efficient due to the indirect bandgap nature of the semiconductor material [12]. The WS_2 films grown from 400 °C substrate temperature was observed three PL emissions at 1.25 eV, 1.78 eV and 1.93 eV. The PL emissions at 1.78 eV and 1.93 eV which are associated with the B and A excitons were attributed to the direct band transitions [13].

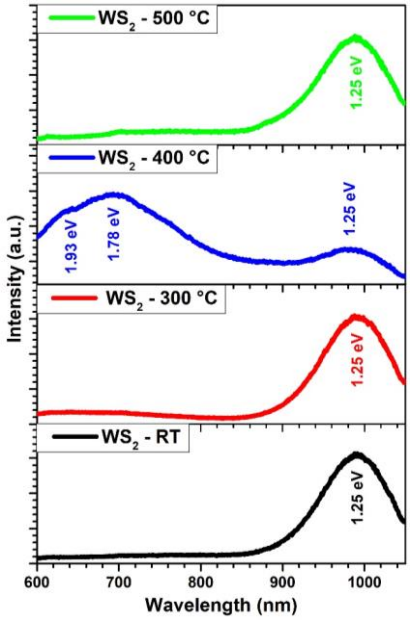

Figure 2. PL spectra of 2D-WS_2

Optical transmission data of 2D-WS_2 films are shown in Figure 3. In Figure 3, the average optical transmission of 2D-WS_2 films in the visible range (400-800 nm) is determined to be 64%, 65%, 78% and 64% for the substrate temperature of RT, 300, 400 and 500 °C respectively. For WS_2 films grown at a substrate temperature of 400°C, the optical transmission indicated a few layers of WS_2 film [14].

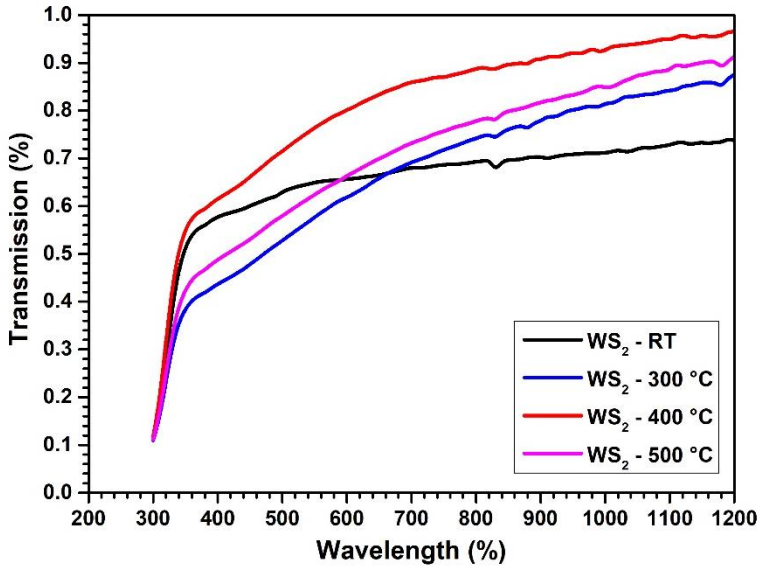

Figure 3. Optical transmission of 2D-WS_2 films

The band gap is an important characteristic of semiconductors, and it determines their electrical and optical properties. The optical properties of the 2D-WS_2 films growth on glass substrate were determined by using the bandgap values calculated from the absorption coefficient obtained by the transmittance spectra of the samples. The bandgap energy values of the samples were calculated by measuring the transmittance spectra with an ellipsometer (J.A. Woollam-VASE) system in our research center. The absorption coefficients of the samples were calculated using the Lambert-Beer law [15] with the measured transmittance values at room temperature in the range of 200-1200 nm and the thicknesses of the WS_2 films.

$$\alpha = \frac{1}{d}\ln\frac{1}{T} \quad (1)$$

The absorption coefficient (α) in Equation (1) represents the absorption coefficient, d represents the thickness of the sample, and T represents the optical transmittance. Using the calculated absorption coefficients with Equation (1), the bandgap energy values of the 2D-WS_2 films were calculated using Equation (2), where E_g is the bandgap energy, A is the constant, hv is the photon energy, and n is the nature of the transition, which takes the value of 1/2 for direct bandgap semiconductors [16].

$$(\alpha hv)^2 = A(hv - E_g) \quad (2)$$

The $(\alpha hv)^2$ - (hv) graph of the samples was plotted (Figure 4) using Equation (2), and the bandgap of the 2D-WS_2 films was determined by identifying the point where the linear part of the curve intersects the hv axis. In the Figure 4, the band gap of the 2D-WS_2 films were determined as 1.85 eV, 2.00 eV, 2.20 eV, and 2.07 eV for RT, 300 °C, 400 °C, and 500 °C substrate temperatures, respectively. In the case of 2D-WS_2 films, the band gap has been reported to be around 2.25 eV for direct band behavior in the literature [12]. It is important to note that the band gap can be affected by various parameters, such as the substrate temperature during growth. In this context, it has been observed that the sample grown at a substrate temperature of 400 °C tends to direct band behavior, whereas the other samples exhibit indirect behaviors.

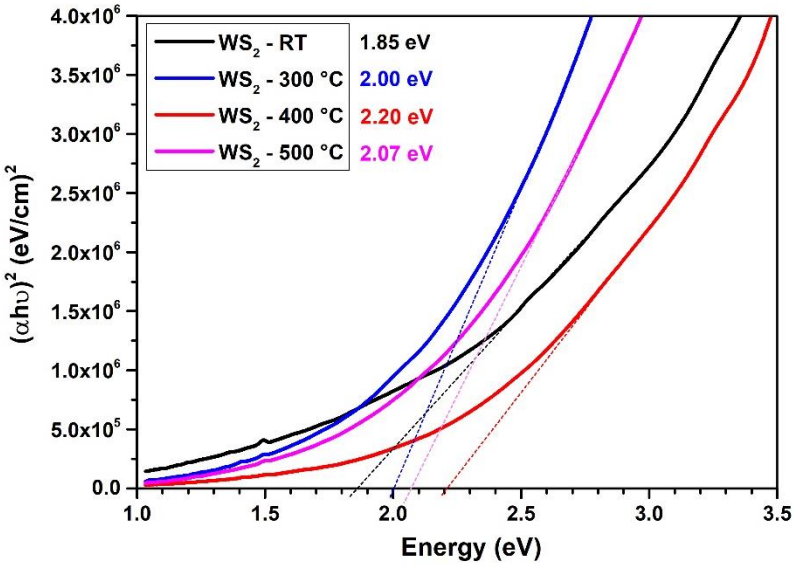

Figure 4. Optical band gap of 2D-WS_2 films.

4. CONCLUSION

In the present study, WS_2 films were grown by PVD method. The different substrate temperatures were considered and 400 °C substrate temperature was determined as the optimum WS_2 growth temperature. According to the Raman and PL spectroscopy measurements of WS_2 films, RT was found to be insufficient for the formation of single phase WS_2 as the obtained film showed bulk structure. With the increase of the substrate temperature, the bulk structure changed into the multilayer structure and the indirect band transition evolved into a direct band transition. Therefore, we conclude that the substrate temperature is highly effective to synthesize high quality WS_2 films by 15 nm WS_2 film at 400 °C. These results enable the use of WS_2 films in optoelectronic applications.

SIMILARITY RATE: 13%

AUTHOR CONTRIBUTION

Ali ALTUNTEPE: Conceptualization, methodology, data curation, writing, editing etc.
Serkan ERKAN: Conceptualization, methodology, data curation, writing, editing etc.
Güldöne KARADENİZ: Characterization.

CONFLICT of INTEREST

The authors declared that they have no known conflict of interest.

REFERENCES

[1] A. Altuntepe *et al.*, "Hybrid transparent conductive electrode structure for solar cell application," vol. 180, pp. 178-185, 2021.
[2] C. Feng, L. Huang, Z. Guo, and H. J. E. c. Liu, "Synthesis of tungsten disulfide (WS2) nanoflakes for lithium ion battery application," vol. 9, no. 1, pp. 119-122, 2007.
[3] B. Luo, G. Liu, and L. J. N. Wang, "Recent advances in 2D materials for photocatalysis," vol. 8, no. 13, pp. 6904-6920, 2016.

[4] S. Tanwar, A. Arya, A. Gaur, and A. J. J. o. P. C. M. Sharma, "Transition metal dichalcogenide (TMDs) electrodes for supercapacitors: a comprehensive review," vol. 33, no. 30, p. 303002, 2021.
[5] C. Cong, J. Shang, Y. Wang, and T. J. A. O. M. Yu, "Optical properties of 2D semiconductor WS2," vol. 6, no. 1, p. 1700767, 2018.
[6] M. Donarelli and L. J. S. Ottaviano, "2D materials for gas sensing applications: a review on graphene oxide, MoS2, WS2 and phosphorene," vol. 18, no. 11, p. 3638, 2018.
[7] C. Lan, C. Li, J. C. Ho, and Y. J. A. E. M. Liu, "2D WS2: from vapor phase synthesis to device applications," vol. 7, no. 7, p. 2000688, 2021.
[8] H. Shi, H. Pan, Y.-W. Zhang, and B. I. J. P. R. B. Yakobson, "Quasiparticle band structures and optical properties of strained monolayer MoS 2 and WS 2," vol. 87, no. 15, p. 155304, 2013.
[9] R. Zan, M. A. Olgar, A. Altuntepe, A. Seyhan, and R. J. R. E. Turan, "Integration of graphene with GZO as TCO layer and its impact on solar cell performance," vol. 181, pp. 1317-1324, 2022.
[10] L. Li, R. Long, and O. V. Prezhdo, "Why chemical vapor deposition grown MoS2 samples outperform physical vapor deposition samples: time-domain ab initio analysis," *Nano letters*, vol. 18, no. 6, pp. 4008-4014, 2018.
[11] M. K. S. Bin Rafiq *et al.*, "WS2: a new window layer material for solar cell application," *Scientific reports*, vol. 10, no. 1, p. 771, 2020.
[12] H. Zeng *et al.*, "Optical signature of symmetry variations and spin-valley coupling in atomically thin tungsten dichalcogenides," vol. 3, no. 1, p. 1608, 2013.
[13] Y. Gao *et al.*, "Large-area synthesis of high-quality and uniform monolayer WS2 on reusable Au foils," *Nature communications*, vol. 6, no. 1, p. 8569, 2015.
[14] Y. Niu *et al.*, "Thickness-dependent differential reflectance spectra of monolayer and few-layer MoS2, MoSe2, WS2 and WSe2," *Nanomaterials*, vol. 8, no. 9, p. 725, 2018.
[15] J. I. Pankove, *Optical processes in semiconductors*. Courier Corporation, 1975.
[16] J. Tauc, "Optical properties and electronic structure of amorphous Ge and Si," *Materials Research Bulletin*, vol. 3, no. 1, pp. 37-46, 1968.